

LATTICE DESIGN OF THE EIC ELECTRON STORAGE RING FOR ENERGIES DOWN TO 5 GeV *

D. Marx[†], J.S. Berg, B. Bhandari, K. Hamdi, D. Holmes, J. Kewisch, Y. Li, Y. Luo, C. Montag, V. Ptitsyn, S. Tepikian, F. Willeke, H. Witte, Brookhaven National Laboratory, Upton, NY, USA
G.H. Hoffstaetter, M.G. Signorelli, Cornell University, Ithaca, NY, USA
B.R. Gamage, Thomas Jefferson National Accelerator Facility, Newport News, VA, USA

Abstract

The Electron-Ion Collider (EIC) at Brookhaven National Laboratory will feature an electron storage ring that will circulate polarized beams with energies up to 18 GeV. Recently a study has been undertaken to extend the minimum energy from 6 GeV to 5 GeV. As the solenoid-based spin rotators around the interaction point require specific bending angles that depend on the energy range, this change results in major changes to the geometry. Moreover, avoiding interference of the electron beamline with the other beamlines in the tunnel, as well as with the tunnel walls, is a formidable challenge, especially at the location of the large-diameter superconducting solenoids. In this contribution, the details of the modified spin rotators, geometrical layout, and optics of the revised lattice are presented.

INTRODUCTION

The Electron-Ion Collider (EIC) [1, 2] is a new machine currently being designed that will collide polarized electrons with polarized hadrons (protons up to heavy ions) for the purpose of investigating the structure and properties of nucleons. It will be built at Brookhaven National Laboratory in the 3.8-kilometer tunnel that currently houses the Relativistic Heavy Ion Collider (RHIC) [3–5]. The two existing RHIC rings will be transformed into a new hadron storage ring, and two new electron rings will be built in this tunnel: a rapid cycling synchrotron (RCS) [6, 7] for accelerating electrons to collision energies and an electron storage ring (ESR) for circulating electron beams for collisions. Figure 1 shows a schematic of the EIC. Collisions will occur at a range of center-of-mass energies between 29 GeV and 140 GeV, providing luminosities up to $10^{34} \text{ cm}^{-2} \text{ s}^{-1}$. These luminosities are considerably greater than those achieved at HERA [5, 8], an electron/positron-proton collider that operated until 2007 at DESY, and, although the top center-of-mass energy will be less than HERA's 318 GeV, the EIC will be optimized for a much wider range of energies. In order to achieve the desired range of center-of-mass energies, various combinations of electron and hadron beam energies will be collided. Three values for the electron beam energy are planned: 5, 10, and 18 GeV.

The ESR lattice consists of six arcs with straight sections in between, labeled according to the numbers on a clock

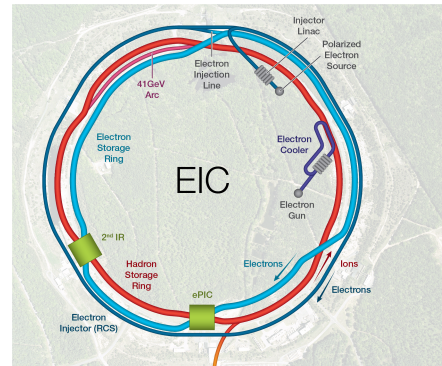


Figure 1: Schematic of EIC (not to scale), showing the main rings that will be installed in the existing RHIC tunnel. The injection complex for the hadrons is not shown here.

face. The baseline design for the EIC includes a single interaction point (IP), called IP6, where the beams will collide. A second IP and detector in the neighboring straight section, IP8, may be included in a future upgrade. Although a simple cross-over beamline will initially be installed at IP8, it is important to consider the design for a full second interaction region, as this sets the path-length requirements [9], and the additional chromaticity generated by this low- β section makes it the most challenging configuration for achieving the required dynamic aperture [10, 11]. The term IP is used to refer to all six points around the clock face between the arcs, even if there are no collisions there. Superconducting RF cavities will be installed at IP10, and the beam will be injected into the ring at IP12.

One of the key requirements for the experimental program is a high level of longitudinal spin polarization. Beams are injected with vertical spin, which is the stable spin direction for the ring. On each side of the IPs, a solenoid-based spin rotator rotates the spin vector into or out of the longitudinal direction. As the spin-rotation angles depend on energy, designing these spin rotators for operation at a wide range of energies is challenging.

Previous versions of the ESR lattice had a lower energy bound of 6 GeV. Recently a study has been performed to investigate extending the energy range down to 5 GeV. This involved changing the bending angles in the spin rotator. In parallel, additional changes to the geometry were made to eliminate interferences with components from other beamlines and the tunnel walls. Due to the limited space available in the tunnel, achieving sufficient clearance between components while fulfilling the geometric requirements of each

* Work supported by Brookhaven Science Associates, LLC, under Contract No. DE-SC0012704 and by Jefferson Science Associates, LLC, under Contract No. DE-AC05-06OR23177 with the U.S. Department of Energy.

[†] dmarx@bnl.gov

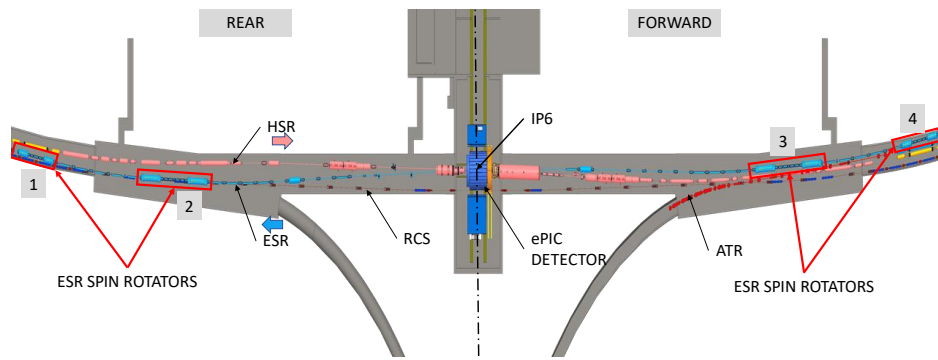


Figure 2: Geometric layout of the interaction region at IP6 with the four solenoid modules shown in red boxes. The RCS lies vertically below the plane of the ESR. The HSR lies in the same plane as the ESR at IP6.

individual beamline is a considerable challenge. This paper provides an overview of the recent changes to the ESR lattice as a result of these efforts.

SPIN ROTATORS

The spin-rotator concept is based on a series of solenoids, dipoles, and matching quadrupoles [12–16], as shown schematically in Fig. 3. The geometric layout in the tunnel is shown in Fig. 2. The tight space constraints owing to the multiple beamlines make the interaction region very challenging. This is especially true for the solenoids, which are strong, superconducting magnets and therefore require significant transverse space for the cryostats. They must fit in the tight space between the HSR and the wall. The specific bending angles required in this section of the ESR constitute additional constraints that make this particularly challenging.

The total bend angle between the short-solenoid module and the IP determines the minimum beam energy for which the spin can be rotated between the vertical and longitudinal axes. With the short solenoids providing $\pi/2$ rotation about the longitudinal axis and the long solenoids turned off, the total bend angle must rotate the spin by $\pi/2$ about the vertical axis. Decreasing the minimum energy from 6 GeV to 5 GeV involves increasing the total bend angle from 116.4 mrad to 136.6 mrad. As the angle between the long-solenoid module and the IP is fixed to 38.8 mrad by the need to rotate the spin by $\pi/2$ at 18 GeV, the bend angle required between the solenoids is now 97.8 mrad. This is accomplished using



Figure 3: The spin rotators are composed of short- and long-solenoid modules, as well as bend modules, to rotate the spin from vertical in the arcs to longitudinal at the IP and back to vertical on the other side.

five 3.8-meter-long dipoles with interleaved quadrupoles. The length of these dipoles is a balance between keeping synchrotron radiation low and fulfilling the tight geometry constraints of this section of the tunnel.

For geometrical reasons it is generally advantageous to minimize the straight lengths of the solenoid modules, which are shown in Fig. 4. The warm quadrupoles between the two solenoids are limited in strength to less than 0.9 T pole-tip field to avoid saturation. The lengths of these quadrupoles have been optimized individually to minimize the total length of the module. Furthermore, the solenoid lengths chosen are a balance between reducing the length of the module and the technical limitations of the magnet. Due to the maturity of the technology and greater choice of vendors, it was desirable to keep the strength limits within the range that may be achieved by NbTi technology. Moreover, there is some trade-off between minimizing the length and the width of the solenoid cryostat. The current design has lengths of 5.5 m for the long solenoids and 1.8 m for the short solenoids with maximum fields of about 8.5 T.

Due to the considerably higher solenoid strengths required, it was decided to give up longitudinal spin matching in the spin rotators. Although the effect on the depolarization time is large, the resulting effect on the bunch replacement time is only about 5 minutes.

GEOMETRY

Overall, the geometric layout of the ESR in the tunnel represents a significant challenge. The total path length of the ESR is fixed such that the revolution time of electrons is equal to that of hadrons in the HSR. Furthermore, the path length between IP6 and IP8 is fixed to allow simultaneous operation of two detectors in the future [9]. For this reason,

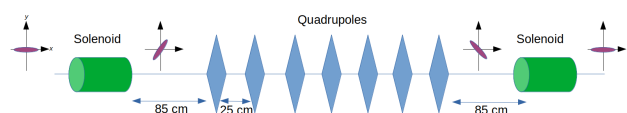


Figure 4: Each solenoid module consists of two half-solenoids with five or seven quadrupoles in between.

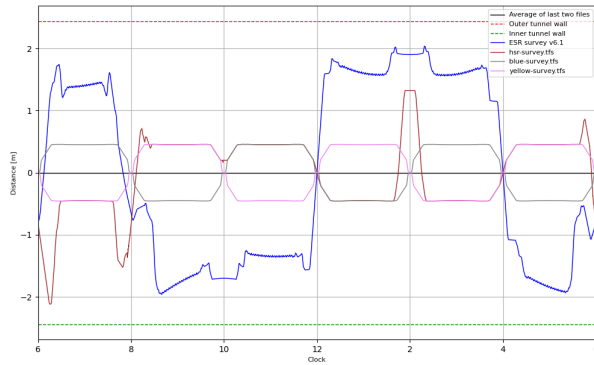


Figure 5: Layout of rings in the tunnel. The horizontal axis shows the angle along the ring, with the labels given in terms of the IP numbers. The vertical axis shows radial distance from the tunnel center, with the red and green dotted lines indicating the tunnel walls. The ESR beamline is shown in blue, alongside the HSR beamline (brown) and the two existing RHIC rings. It is planned to remove parts of the RHIC rings that are not being used in order to eliminate interferences.

the lattice with two collision points is considered in the first instance, even though this will not be the initial configuration to be built.

To maintain some symmetry of the ring, the total bend angle of the spin rotators is repeated in the other straight sections (which, despite their name, contain some dipoles). Decreasing the minimum energy of 6 GeV to 5 GeV has therefore decreased the bend angle in the arc cells and increased the bend angle in the straight sections. As a consequence the arc dipoles have also decreased in length with more space given to the straight sections.

Beamline elements must be carefully placed to avoid interferences with other beamlines and the tunnel walls. The solenoids are particularly challenging due to their considerable width in a tight section of the beamline, but there are many other locations where magnets are very close to either the walls or other beamlines. Much work has been done to eliminate such interferences, primarily by adjusting the geometry of the ESR by means of varying drift lengths and dipole angles, but also modifying other beamlines and considering the use of alternative magnets. Figure 5 shows a representation of the geometry layout of the whole ring.

OPTICS

Figure 6 shows the matched optics for the 18 GeV lattice with two collision points. Table 1 shows the main lattice parameters at 18 GeV with 1 and 2 IPs. The two lattices are identical with two full interaction regions; however, for the 1 IP lattice the β functions are additionally squeezed at IP8. This results in a smaller natural chromaticity for the 1 IP lattice.

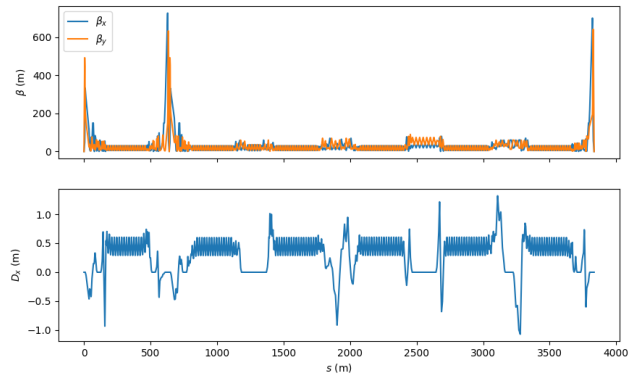


Figure 6: β functions and dispersion for matched ring with 2 IPs.

Table 1: ESR Lattice Parameters at 18 GeV with 1 and 2 IPs

| Parameter | 1 IP | 2 IP |
|----------------------------|---------------|---------------|
| Arc cell phase adv. | 90° | 90° |
| Hor. emit. (nm) | 24 | 25 |
| Energy spread | 0.095% | 0.095% |
| β_x^*/β_y^* (m) | 0.59 / 0.057 | 0.59 / 0.057 |
| Tunes, Q_x/Q_y | 50.08 / 44.14 | 50.08 / 44.14 |
| Nat. chrom., ξ_x/ξ_y | -92 / -92 | -108 / -117 |

The optics are periodic in the arcs, with the phase advance set to 90° at 18 GeV and 60° at 5 and 10 GeV. There is also some periodicity in the straight sections, primarily to reduce the number of required power supplies. The phase advances between arcs will be used as variables in the optimization of the dynamic aperture [10, 11], so these are expected to change from the current linear optics match shown here. The global tune is fixed and was chosen to be suitable for beam-beam as well as polarization performance [17].

CONCLUSION

Recently, much work has been performed to update the ESR lattice design. A major change is the change in geometry of the spin rotators necessary to provide longitudinally polarized electrons at collision down to energies of 5 GeV. Many modifications have been made to avoid interferences with other beamlines and with the tunnel walls. Magnet lengths have been chosen with regard to reducing the number of new magnets that will have to be designed and built, and reusing existing magnets from other facilities where possible.

There is further work to be done, especially on the design of the crossover at IR8 and redesigning the straight section at IR4 to eliminate interferences. Local coupling correction in the interaction region at IP6 needs to be incorporated into the lattice, as well as a scheme to generate coupling between the transverse planes in order to increase the vertical emittance. Furthermore, locations of collimators, correctors, and diagnostics need to be settled on.

REFERENCES

- [1] J. Beebe-Wang *et al.*, “Electron-Ion Collider: Conceptual Design Report,” 2021.
- [2] C. Montag *et al.*, “Design Status of the Electron-Ion Collider”, presented at the IPAC’23, Venice, Italy, May 2023, paper MOPA049, this conference.
- [3] C. Montag, “RHIC status and plans,” *AIP Conference Proceedings*, vol. 2160, no. 1, p. 040006, 2019.
doi:10.1109/PAC.2003.1288831
- [4] “RHIC Configuration Manual,” 2006.
- [5] K. Hübner, S. Ivanov, R. Steerenberg, T. Roser, J. Seeman, K. Oide, K. H. Mess, P. Schmüser, R. Bailey, and J. Wenninger, “The largest accelerators and colliders of their time,” in *Particle Physics Reference Library : Volume 3: Accelerators and Colliders* (S. Myers and H. Schopper, eds.), Springer.
- [6] V. Ranjbar *et al.*, “Progress on the Electron Ion Collider’s RCS RF ramp development”, presented at the IPAC’23, Venice, Italy, May 2023, paper MOPA035, this conference.
- [7] H. Lovelace III, F. Lin, V. Ranjbar, and C. Montag, “The Impact of Magnetic Errors on the Electron Ion Collider Rapid Cycling Synchrotron”, presented at the IPAC’23, Venice, Italy, May 2023, paper WEPL088, this conference.
- [8] National Academies of Sciences, Engineering, and Medicine, “An Assessment of U.S.-Based Electron-Ion Collider Science,” National Academies Press, 2018.
doi:10.17226/25171
- [9] J. Berg *et al.*, “Synchronizing the Timing of the Electron and Hadron Storage Rings in the Electron-Ion Collider”, presented at the IPAC’23, Venice, Italy, May 2023, paper MOPL157, this conference.
- [10] Y. Cai, Y. Nosochkov, J. S. Berg, J. Kewisch, Y. Li, D. Marx, C. Montag, S. Tepikian, F. Willeke, G. Hoffstaetter, and J. Unger, “Optimization of chromatic optics in the electron storage ring of the electron-ion collider,” *Phys. Rev. Accel. Beams*, vol. 25, p. 071001, Jul 2022.
doi:10.1103/PhysRevAccelBeams.25.071001
- [11] Y. Nosochkov *et al.*, “Dynamic Aperture Studies for the EIC Electron Storage Ring,” Venice, Italy, May 2023, 14, presented at IPAC’23, Venice, Italy, May 2023, paper MOPA048, this conference.
- [12] D. Marx *et al.*, “Designing the eic electron storage ring lattice for a wide energy range,” *Journal of Physics: Conference Series*, vol. 2420, p. 012010, 2023.
doi:10.1088/1742-6596/2420/1/012010
- [13] D. Marx *et al.*, “Task Force Report: ESR Linear Lattice Design”, No. EIC-ADD-TN-025, BNL-222485-2021-TECH., Brookhaven National Lab.(BNL), Upton, NY (United States), 2021.
- [14] D. Barber *et al.*, “A solenoid spin rotator for large electron storage rings,” *Particle Accelerators*, vol. 17, pp. 243–262, 1985.
- [15] P. Emma, “A spin rotator system for the NLC,” SLAC, USA, SLAC NLC-Note-07, 1994.
- [16] V. Ptitsin and Y. Shatunov, “Siberian Snakes for Electron Storage Rings”, in *Proc. PAC’97*, Vancouver, Canada, May 1997, paper 9P022, pp. 3500-3502.
- [17] Y. Luo *et al.*, “Optimizing the Design Tunes of the Electron Storage Ring of the Electron-Ion Collider,” Venice, Italy, May 2023, 14, presented at IPAC’23, Venice, Italy, May 2023, paper MOPA047, this conference.